

The Influences of Stellar Activity on Planetary Atmospheres

Colin P. Johnstone

University of Vienna, Department of Astrophysics, Türkenschanzstrasse 17, 1180 Vienna, Austria

email: colin.johnstone@univie.ac.at

Abstract. On evolutionary timescales, the atmospheres of planets evolve due to interactions with the planet's surface and with the planet's host star. Stellar X-ray and EUV (= 'XUV') radiation is absorbed high in the atmosphere, driving photochemistry, heating the gas, and causing atmospheric expansion and mass loss. Atmospheres can interact strongly with the stellar winds, leading to additional mass loss. In this review, I summarise some of the ways in which stellar output can influence the atmospheres of planets. I will discuss the importance of simultaneously understanding the evolution of the star's output and the time dependent properties of the planet's atmosphere.

1. Introduction

Energy released in the cores of stars is transferred into the stellar environment by a multitude of different processes. These include emission of infrared, visible, and ultraviolet light from the star's photosphere, emission of far ultraviolet (FUV), extreme ultraviolet (EUV) and X-rays from the chromosphere and corona, the acceleration of supersonic winds and coronal mass ejections, and the ejection of high energy protons and electrons. Nearby planets are embedded in this environment and are influenced in radically different ways by each of these different processes. In many cases, stellar output causes a variety of atmospheric loss processes, influencing the evolution of the planet's atmosphere. In this review, I will discuss the various manifestations of stellar activity and the resulting losses from planetary atmospheres.

Planets that form to a significant mass within a few Myr of the start of system can gravitationally attract a thick envelope from the circumstellar gas disk; these atmospheres are often called 'primordial atmospheres'. In such cases, the atmospheres are primarily composed of Hydrogen and Helium and can have masses that are a few percent of the planet's own mass, with surface temperatures of several thousand K. Regardless of whether or not they form to large enough masses to gain a primordial atmosphere, bodies of all sizes that form in the disk trap heavier volatile species such as nitrogen, oxygen, and carbon dioxide. After the circumstellar gas disk is gone, terrestrial planets form through the accretion of such bodies. These volatiles can be released when the bodies impact with a forming planet, to form an atmosphere or contribute to an existing atmosphere. Volatile elements that are not released during impacts, or were trapped in the planet as it first formed, can then be released both as the magma ocean that likely exists in the early phases of planet formation solidifies (Elkins-Tanton 2008) and from volcanoes in later phases. Atmospheres formed after the disk phase, i.e. non-primordial atmospheres, can have a range of compositions, with H₂O (e.g. possibly early Venus), CO₂ (e.g. current Venus and Mars), and N₂ (e.g. current Earth) being possible dominant species. In all cases, the later atmospheric evolution can be determined by interactions with the planet's host star.

In this review, I discuss some of the influences that stellar activity related phenomena can have on planetary atmospheres. Given the limited scope of this review, the reader should be aware that there are many interesting and important processes that are not mentioned here. In Section 2, I summarise some of the various phenomena that are part of ‘stellar activity’ and how they evolve; in Section 3, I discuss the influences of stellar activity on planetary atmospheres; in Section 4, the evolution of primordial atmospheres; finally, in Section 5, I give some final remarks.

2. The various manifestations of stellar activity

In this review, I am interested in the effects of stellar ‘activity’, i.e. phenomena related to the star’s magnetic field. The magnetic field provides a route by which convective energy in the star’s photosphere can be transferred upwards and deposited in the overlying layers. The resulting heating leads to gas at EUV and X-ray emitting temperatures, and the acceleration of gas away from the star in the form of a stellar wind.

2.1. Emission of EUV and X-rays

Starting in the solar photosphere with a temperature of ~ 6000 K, the temperature first decreases with increasing height until it reaches a minimum in the chromosphere. At higher altitudes, the temperature first increases in the chromosphere and then shoots up in the transition region to MK temperatures in the corona, as shown in the upper panel of Fig. 1. The plasma in these different layers emit at very different wavelengths. The photosphere dominates in the visible, ultraviolet, and infrared with an approximately blackbody spectrum. The chromosphere mostly emits at far ultraviolet and extreme ultraviolet wavelengths and the corona emits at extreme ultraviolet and X-ray wavelengths. As can be seen in Fig. 10 of Fontenla *et al.* (2009), chromospheric emission dominates at wavelengths of 500 \AA and longer and coronal emission dominates at shorter wavelengths. The solar spectrum is shown in Fig. 1.

The chromospheric and coronal heating mechanisms have not yet been unambiguously identified. It is clear, however, that the heating is directly a result of the magnetic field. For example, Pevtsov *et al.* (2003) showed that various features on the solar surface, such as active regions, have a very tight relation between magnetic flux in the photosphere and X-ray luminosity which is valid over many orders of magnitude. Over the course of the solar cycle, the magnetic flux, and therefore the EUV and X-ray emission varies, by large amounts. Pevtsov *et al.* (2003) also showed that their solar relation holds when going to young active stars that have orders of magnitude higher X-ray luminosities.

Observations of other stars in X-rays have shown that similar processes are operating on stars with masses similar to or less than that of the Sun. Unfortunately, interstellar absorption makes it very difficult to observe EUV from stars, and only a few observations exist for the nearest stars. The general trend is that the X-ray luminosity, L_X , is higher for stars that rotate faster, up until a certain rotation rate where the L_X -rotation relation saturates. The saturation threshold happens approximately at a constant value of $L_X/L_{\text{bol}} \sim -3$ (Pizzolato *et al.* 2003). The rotation rate at which stars saturate in X-rays depends strongly on mass, with a value of $\sim 15\Omega_{\odot}$ for solar mass stars and values of $\sim 1\Omega_{\odot}$ for M dwarfs. This means that lower mass stars (e.g. M dwarfs) never become as active as the most active solar mass stars. Observationally, it is known that the coronal temperature depends sensitively on its activity level (e.g. Johnstone & Güdel 2015), which means that the X-ray spectrum is generally shifted to shorter wavelengths (Güdel *et al.* 1997). We also expect significantly different spectra for lower mass stars, such as M dwarfs, especially in the near ultraviolet (see Fig. 9 of Fontenla *et al.* 2016).

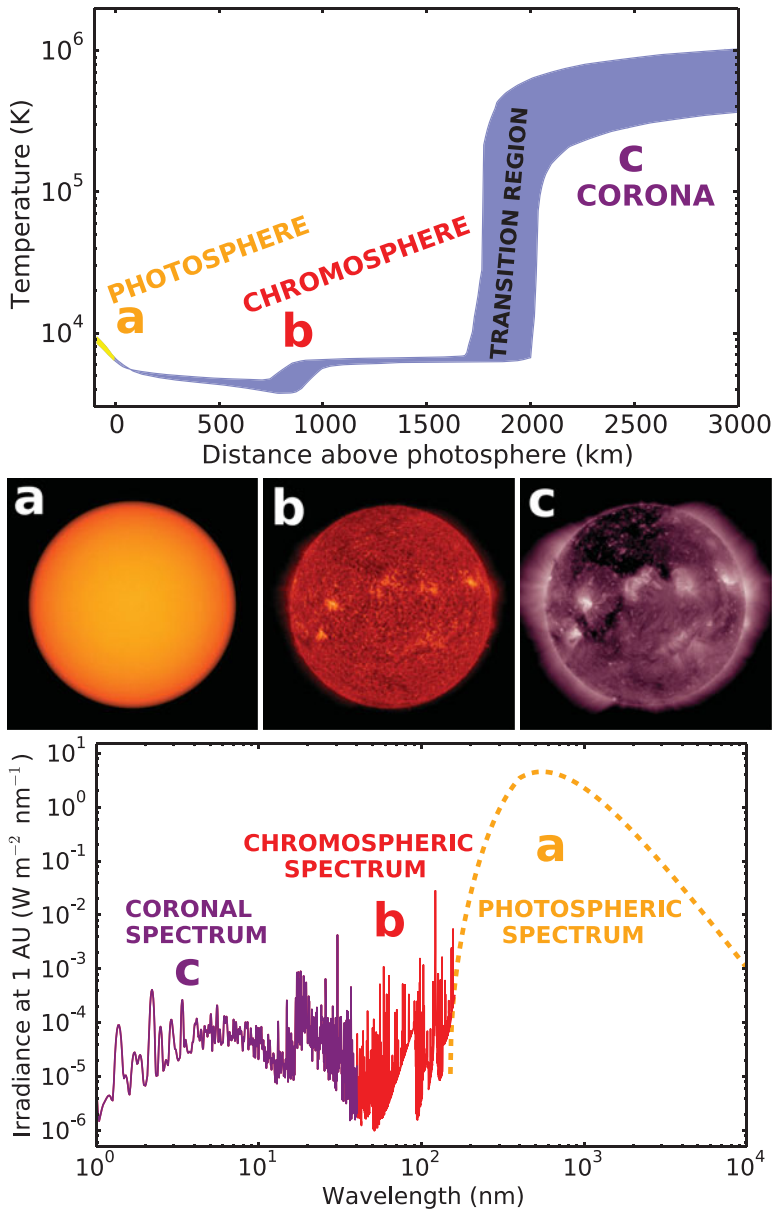


Figure 1. Figure showing the heating and emission of the solar atmosphere. *Upper panel:* the temperature structure of the chromosphere, transition region, and corona. The areas represent a range of temperatures for different features in the solar atmosphere, as shown in Fig. 1 of Fontenla *et al.* (2011). *Middle panel:* images of the Sun from the Solar Dynamics Observatory (SDO) showing the Sun at different wavelengths courtesy of NASA/SDO and the AIA, EVE, and HMI science teams. The three panels show plasmas with different temperatures, and therefore different heights in the solar atmosphere and contribute differently to the solar spectrum; they show (a) the photosphere at ~ 5800 K, (b) the chromosphere and transition region at $\sim 5 \times 10^4$ K, and (c) the corona at ~ 2 MK. *Lower panel:* the solar spectrum between 1 nm and 10^4 nm. The various parts are from the solar photosphere (dashed yellow line), the primarily chromospheric dominated spectrum up to 500 nm (red line), and the primarily coronal dominated spectrum at longer wavelengths (purple line). The chromospheric and coronal spectra were calculated by Fontenla *et al.* (2011).

2.2. Winds and coronal mass ejections

The stellar wind heating and acceleration mechanisms are currently poorly understood. The most likely mechanism is energy and momentum deposition by waves (e.g. Alfvén waves) produced in the photosphere that propagate upwards along magnetic field lines. Alternatively, injections of mass and energy into the wind by magnetic reconnection events near the surface might play a role. For a review, see Cranmer (2009).

As a simple approximation, the wind breaks down into three components: these are the slow wind, the fast wind, and coronal mass ejections (CMEs). The slow and fast components are both relatively steady streams of particles, with similar mass fluxes, that are distinguished based primarily on their outflow speeds, with average values of $\sim 400 \text{ km s}^{-1}$ and $\sim 800 \text{ km s}^{-1}$ respectively. The spatial distributions of slow and fast winds depend sensitively on the structure of the global magnetic field in the corona, with fast wind originating from the centres of coronal holes (regions where the magnetic field lines are ‘open’) and slow wind dominating in regions above closed magnetic fields. For the slow wind, the main open question is the exact spatial origin in the corona[†]. A difficulty for the fast wind is the fact that measurements of the wind temperatures in the corona show that the wind is not hot enough to be accelerated to $\sim 800 \text{ km s}^{-1}$ by thermal pressure alone, and therefore other acceleration mechanisms must be invoked.

Although the bulk properties of the solar wind are known in a lot of detail, very little is known about the bulk properties of the winds of other low-mass stars, and nothing is known with any certainty. Several studies have attempted to constrain wind properties observationally, using for example radio emission (e.g. Gaidos *et al.* 2000), astrospheric absorption of Ly α radiation (Wood *et al.* 2014), and planetary transits (Kislyakova *et al.* 2014b). Johnstone *et al.* (2015b) estimated a scaling law for wind mass loss rates of $\dot{M}_* \propto R_*^2 \Omega_*^{1.33} M_*^{-3.36}$ by fitting a rotational evolution model to observational constraints. Stellar spin down on the main-sequence is probably the most unambiguous and well constrained observational signature of stellar winds, though using it to derive wind properties is difficult (see Section 4.3 of Johnstone *et al.* 2015b). Many stellar wind models have been developed and applied: these include theoretical models that consider energy balance in the transition region (Cranmer & Saar 2011), hydrodynamic models of the solar wind scaled to the winds of other stars (e.g. Johnstone *et al.* 2015a), and 3D magnetohydrodynamic (MHD) models based on observed magnetic field geometries (e.g. Vidotto *et al.* 2015). Recently, more physically based MHD models have been applied that heat and accelerate the wind using Alfvén waves (van der Holst *et al.* 2014; Airapetian & Usmanov 2016; Cohen *et al.* 2016), though there are still uncertainties and free parameters in these models. I should also note that for the most rapidly rotating stars, the wind acceleration can be dominated by magneto-centrifugal forces; such winds can have speeds far from the star of several thousand km s^{-1} (Johnstone 2016). For a review of stellar wind observations and models, see Section 2 of Johnstone *et al.* (2015a).

Coronal mass ejections are clouds of coronal plasma that are released by the corona and accelerated at speeds that range from slower than the solar wind up to several thousand km s^{-1} . On the Sun, they are known to be correlated with flares, with the most massive flares almost always being accompanied by a CME (Wang & Zhang (2007)). The CME rate generally varied with the solar cycle, reaching up to a ten per day at cycle maximum

[†] The most natural possibility is that the slow wind comes from the edges of coronal holes and is directed by the magnetic field into the regions above closed field lines. Alternatively, the slow wind could come from closed field regions, and is released into the wind through diffusion of material across field lines or through magnetic reconnection at the closed/open field boundaries and the tops of helmet streamers. For a recent review on the subject, see Abbo *et al.* (2016).

(Robbrecht *et al.* 2009). On other stars, CMEs have not been unambiguously detected, but the relation between flares and CMEs indicate that more active stars release CMEs at higher rates (Aarnio *et al.* 2012). It could be that the winds of active stars are in fact dominated by CMEs, though it is currently not known if this is indeed the case.

2.3. Evolution of stellar activity

Given the empirical relation between X-ray emission and rotation, and the likely relation between winds and rotation, it is natural to assume that the evolution of stellar activity is mostly a result of rotational evolution. Stars are born with rotation rates anywhere between a few times to a few tens of times the rotation rate of the Sun ($\Omega_{\odot} \approx 2.9 \times 10^{-6} \text{ rad s}^{-1}$). As they contract on the pre-main-sequence, they spin up (i.e. their rotation rates increase with time) until just before they reach the zero-age main-sequence (ZAMS). After the ZAMS, the dominant effect is angular momentum removal by stellar winds, causing them to spin down. The initial wide distribution of rotation rates gets wider when spinning up and then converges to a single mass and age independent value early on the main-sequence. The convergence time depends very much on stellar mass, with solar mass stars taking ~ 750 Myr to converge fully and lower mass stars taking longer. For M dwarfs, it is possible that a subset of stars do not converge at all and remain rapidly rotating. For a review of stellar rotational evolution, see Bouvier *et al.* (2014).

Spin down results in stellar activity decreasing with age. For solar analogues, this decay in X-rays is approximately $L_X \propto t^{-1.5}$ (Güdel *et al.* 1997). For longer wavelengths, this decay is less steep (Ribas *et al.* 2005). These single time dependent decay laws are however only valid after rotational convergence has taken place. Tu *et al.* (2015) used a rotational evolution model to estimate the different evolutionary tracks for stellar X-ray and EUV emission and showed that these tracks fit very well the distributions of X-ray emission observed in young clusters. Their evolutionary tracks for rotation and XUV emission are shown in Fig. 2. Although it is not known, it is natural to expect that stellar winds also follow different evolutionary tracks for different rotational evolutions. Such tracks were estimated by Johnstone *et al.* (2015b) using $\dot{M}_{\star} \propto \Omega_{\star}^{1.33}$, i.e. the relation mentioned in the previous section applied to solar mass and radius stars. I show these evolutionary tracks for the solar wind in time in Fig. 3, as well as a similar estimate calculated assuming $\dot{M}_{\star} \propto \Omega_{\star}^{2.43}$ which I estimated for this review based on the wind models of Airapetian & Usmanov (2016). Clearly, our uncertainties for the properties of the early solar wind come from two sources: our lack of knowledge of the relevant wind physics and our lack of knowledge of how rapidly the Sun was rotating. Given that low mass stars often remain rapidly rotating for longer, and the saturation rotation rate is lower (so that even relatively slowly rotating M dwarfs can be highly active), low mass stars remain active for much longer than solar mass stars (West *et al.* 2008).

3. Activity driven atmospheric losses

Atmospheric losses driven by stellar XUV radiation, winds, and high energy particles have been observed both in our own solar system (Lammer *et al.* 2009) and in the transits signatures of planets orbiting other stars (Ehrenreich *et al.* 2008; Kislyakova *et al.* 2014b). To first approximation, the majority of planetary mass loss mechanisms can be broken down into two categories: ‘thermal’ and ‘non-thermal’. Thermal loss mechanisms are those that are directly a result of the heating of the planetary atmosphere and non-thermal mechanisms are essentially all other processes. In this section, I will instead break down these mechanisms into radiation induced and wind induced losses.

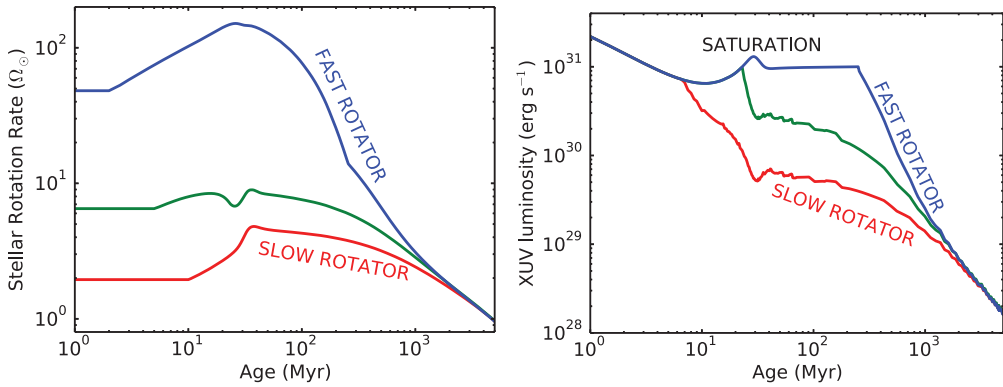


Figure 2. Figure showing the evolution of rotation (*left panel*) and XUV (*right panel*) for solar mass stars with different initial rotation rates, calculated by Tu *et al.* (2015).

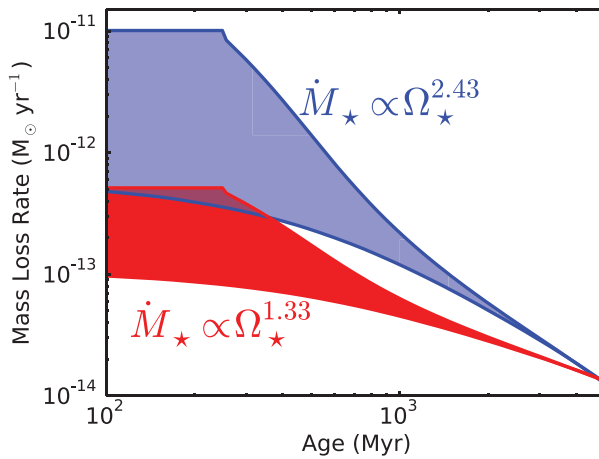


Figure 3. Figure showing the evolution of the mass loss rates of solar mass stars from 100 Myr to 5 Gyr assuming that $\dot{M}_\star \propto \Omega_\star^a$ for two different values of a . The value of $a = 1.33$ was estimated by Johnstone *et al.* (2015b) and the value of $a = 2.43$ is the largest value that can be derived based on the results of the wind models of Airapetian & Usmanov (2016). The upper and lower limits of each shaded areas are the tracks for fast and slow rotating stars respectively.

3.1. Atmospheric losses due to stellar radiation

There are several ways in which the various layers in the Earth’s atmosphere can be broken down; the most common of these is by temperature gradient. Starting at the surface and going to higher altitudes, the temperature first decreases in the troposphere, then increases in the stratosphere due to absorption of solar UV by ozone, and then decreases again in the mesosphere due to the increasing importance of cooling by CO₂. Above the mesosphere is the thermosphere, where the absorption of solar X-ray and EUV radiation causes the temperature to increase to a few thousand K. Solar radiation also ionises the upper atmosphere, creating the ionosphere, which corresponds to the upper mesosphere and the thermosphere. In general, higher input XUV fluxes lead to a hotter and more expanded thermosphere. The response of the Earth’s current atmosphere to increased XUV irradiation was studied by Tian *et al.* (2008) and is summarised in Fig. 4.

The gas in the thermosphere is essentially hydrostatic and as we go to higher altitudes, the particle density decreases rapidly. Eventually, the density becomes so low that

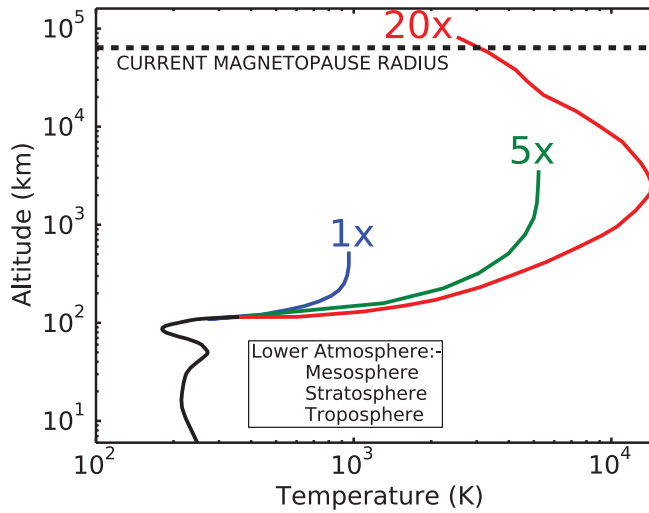


Figure 4. Figure showing how the thermosphere of the Earth reacts to different XUV fluxes (where 5x for example indicated five times what the Earth currently gets on average), adapted from Fig. 6 of Tian *et al.* (2008). Each line stops at the exobase. Adiabatic cooling can be seen in the 20x case due to the wind flowing away from the planet.

particles can travel a large distance without interacting with each other. The thermosphere ends at the point where the gas becomes essentially collisionless; this is the exobase, above which the particles travel on ballistic trajectories. Particles that have upward velocity components that are higher than the escape speed are lost from the atmosphere; this loss mechanism is called Jeans escape. The Jeans escape rate depends sensitively on the altitude and gas temperature of the exobase; another important factor is the molecular mass of the species, with lighter species escaping easier than heavier species.

A useful parameter to calculate at the exobase is the Jeans escape parameter, given by $\lambda_J = GM_p m / k_B T_{\text{exo}} R_{\text{exo}}$, where m is the molecular mass of the species being considered, and T_{exo} and R_{exo} are the temperature and radius of the exobase respectively. This is simply the ratio of the potential energy to the kinetic energy at the exobase. When λ_J is relatively high, the atmosphere is approximately hydrostatic and the main thermal loss mechanism is Jeans escape, with a mass loss rate that depends strongly on λ_J . When λ_J is close to unity, the atmosphere is not hydrostatic, but has enough energy to flow away from the planet as a planetary wind. In Fig. 5, I show some hydrodynamic simulations from Johnstone *et al.* (2015b) of the planetary wind of an Earth mass planet with a hydrogen dominated envelope under different X-ray and EUV conditions. The winds start out subsonic low in the thermosphere, and as the temperature rises due to XUV heating, the winds accelerate to supersonic speeds. Like any Parker wind, the radius at which the winds become supersonic is the same as the radius at which their outflow speed becomes equal to the escape velocity. This means that in the supersonic part of the wind, the material will be lost from the planet, regardless of other effects such as additional heating or stellar wind pick-up. A fundamental requirement for a hydrodynamically outflowing wind is that it becomes supersonic before the exobase, otherwise the particles that move up into the exosphere will mostly not have reached escape velocity.

3.2. Atmospheric losses due to stellar winds/CMEs

Stellar winds bring with them a large amount of energy and momentum, which can be given to the atmosphere below the exobase or to individual atmospheric particles in the

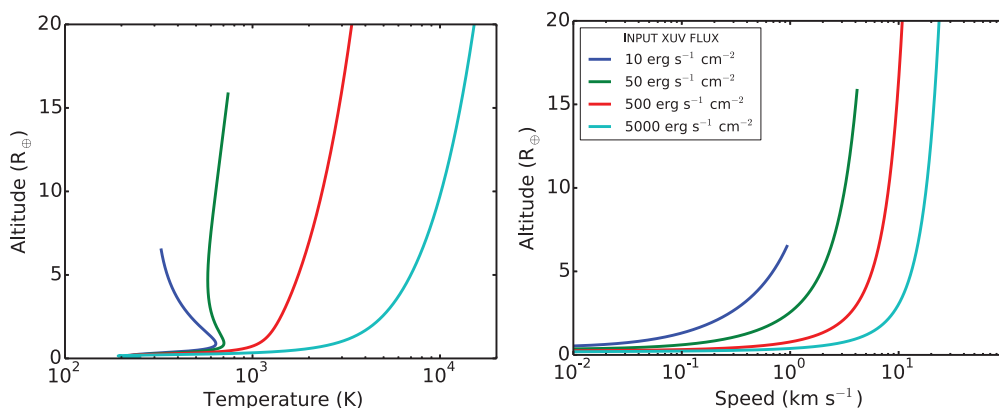


Figure 5. Figure showing the thermospheric temperature and velocity structure a hydrogen dominated atmosphere undergoing hydrodynamic escape with different input XUV fluxes, reproduced from Johnstone *et al.* (2015b).

exosphere. The planetary magnetosphere can play an important role in determining how the wind and the atmosphere interact; they can both protect atmospheres by shielding them from interacting directly with winds, and expose atmospheres more by increasing the effective area of the planet that can collect wind energy and momentum.

Stellar wind/CME protons and electrons can directly enter the atmosphere; for a magnetised planet, this will take place at the magnetic poles. Their effects on the atmosphere include ionisation and heating, which can lead to increased outflow (e.g. Glocer *et al.* 2009). In addition, wind particles that collide with atmospheric particles give them their momentum directly which can lead to the atmospheric particles escaping the planet, or giving this momentum to other atmospheric particles that then escape (Johnson 1994). This effect is called ‘sputtering’.

Winds can also pick up atmospheric particles in the exosphere. In order to be picked up, an atmospheric particle should first be ionized so that it can interact with the magnetic field in the wind. Several mechanisms exist that can ionize a particle if it is not already ionized lower in the atmosphere: these include photoionisation from a stellar XUV photon, electron-impact ionisation from a stellar wind electron, and charge exchange. Charge exchange involves a supersonic stellar wind proton taking an electron from a slow atmospheric particle, resulting in an atmospheric ion and a supersonic neutral Hydrogen atom. Heavier ions can also undergo charge exchange, often resulting in the ion emitting an X-ray photon, which itself can be an additional source of X-ray irradiation of the planet (Kislyakova *et al.* 2015). The atmospheric ions that are produced can either be lost from the planet entirely (e.g. Kislyakova *et al.* 2014a) or be accelerated back into the planet’s atmosphere or magnetosphere, potentially increasing the heating and causing additional sputtering (Luhmann & Kozyra 1991).

The high-speed Hydrogen atoms that are produced as a result of charge exchange are called an energetic neutral atoms (ENAs). ENAs can fly unhindered through a planet’s magnetic field and deposit their energy in the atmosphere. This was suggested as a significant heating mechanism in the upper atmosphere of early Venus by Chassefière (1997). Recently, Lichtenegger *et al.* (2016) studied this process for early Venus, assuming that the planet had a water vapour atmosphere that was undergoing hydrodynamic escape because of the early Sun’s high activity levels. They found that while ENAs bring in a significant energy, the energy is deposited high up in the atmosphere, after the

planetary wind had already accelerated to a significant speed, and therefore the heating did not influence the atmospheric loss rates significantly.

There are several other ways in which winds can give energy to planetary atmospheres. For example, wind-magnetospheric interactions can generate electric currents in the ionosphere which then release energy due to Joule heating. This was studied by Cohen *et al.* (2015) for planets in the habitable zones of low mass stars. In this case, planets are expected to be embedded in dense winds because of the close-in habitable zones, and therefore the heating rate from Joule heating is likely much larger.

4. Evolution of primordial atmospheres orbiting active stars

Primordial atmospheres are picked up by planets that form fast enough to have significant masses ($\gtrsim 0.1M_{\oplus}$) during the gas disk phases of their systems (i.e. within a few Myr). Lammer *et al.* (2014) and Stökl *et al.* (2016) showed that the mass of the obtained atmosphere depends sensitively on the mass of the planet, with $5.0M_{\oplus}$ planets picking up atmosphere that are a factor of 10^5 larger than those picked up by $0.1M_{\oplus}$ planets (see Table 2 of Stökl *et al.* 2016 and the lower panels of Fig.6). However, significant uncertainty exists in how much atmosphere is gained, largely due to its sensitivity on the energy input into the atmosphere and the how quickly this energy can be radiated away[†]. Of course, we also shouldn't forget that planet's likely undergo significant growth after the disk phase (e.g. the Earth was likely only half its current mass 10 Myr after solar system formation; see Table 6 of Kleine *et al.* 2009), and we won't know for any given planet that we observe what its mass was at the end of the disk phase.

Stökl *et al.* (2015) studied the evolution of these atmospheres after the gas disk dissipated, assuming the planets were located at 1 AU; they found that after the gas disk dissipates, the primordial atmospheres of low mass ($\lesssim 0.5M_{\oplus}$) planets would quickly flow away, even without additional XUV heating. Similarly, Owen & Wu (2016) studied this for planets at much smaller orbital distances from their host stars who found that due to the much stronger irradiation from the star's photospheric spectrum, even super-Earths will lose most of their atmospheres after disk dispersal. Lammer *et al.* (2014) combined estimates of the pick up of primordial atmospheres with models for the XUV driven hydrodynamic atmospheric losses and found that planets with masses less than that of the Earth likely lose their primordial atmospheres and planets more massive than the Earth keep them. Similar results were found by Owen & Mohanty (2016), who instead considered terrestrial planets in the habitable zones of M dwarfs. In both cases, the high levels of atmospheric loss are a result of the star's high X-ray and EUV luminosities. These results suggest that we should expect to find many planets with H/He-dominated primordial atmospheres, with the exceptions being planets with masses $\lesssim 1.0M_{\oplus}$, and more massive planets that either formed after the dissipation of the gas disk or are on close orbits around their host stars. The observational situation currently appears to support the conclusion that super-Earths mostly have low densities, implying that they have H/He envelopes (Rogers 2015).

Given that atmospheric losses are closely dependent on the star's activity level, it is important that stellar activity evolution is properly taken into account when studying atmospheric evolution (at least when this evolution is a result of losses into space and not

[†] It is useful to picture the pick up of a protoatmosphere in the gas disk by a terrestrial planet as being analogous to the contraction of a star on the pre-main-sequence and not analogous to the planet sucking up the atmosphere around it like a vacuum cleaner. Essentially, the disk gas is contracting around the gravitating body and this contraction rate depends sensitively on the rate at which the thermally-supported atmosphere can cool.

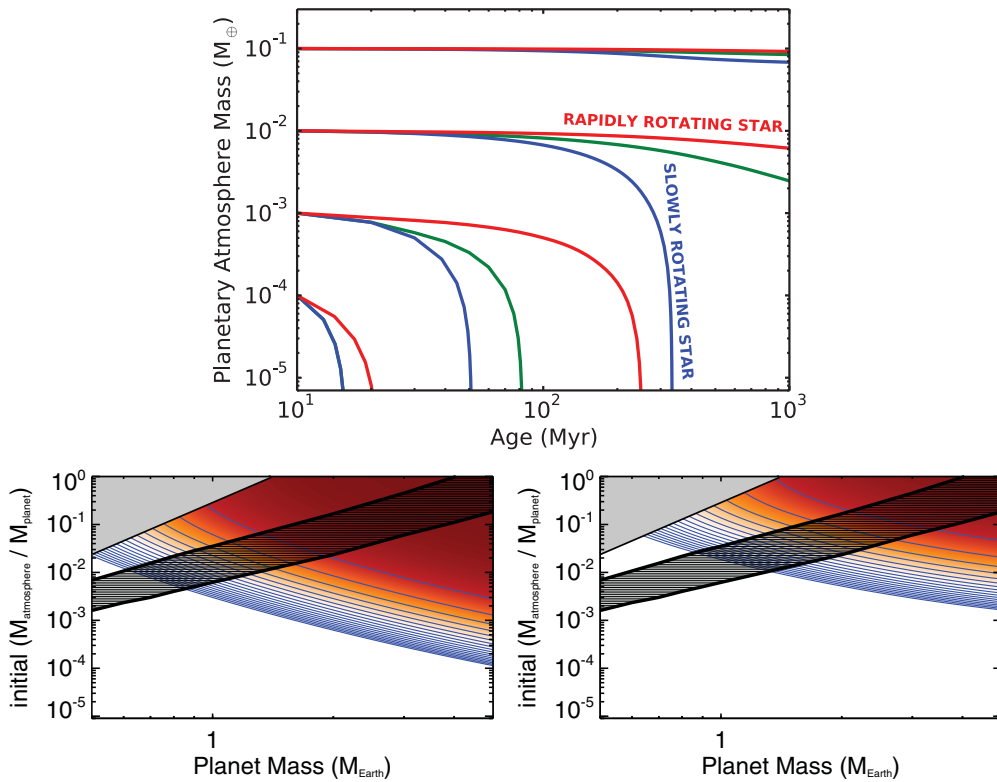


Figure 6. Figure showing the results of Johnstone *et al.* (2015b) for terrestrial planets with H/He dominated primordial atmospheres orbiting at 1 AU around a solar mass star. *Upper-panel:* atmospheric evolution with four different initial starting atmospheric masses; for each case, the red, green, and blue lines correspond to the slow, medium, and fast rotator cases for the host star. *Lower-panels:* remaining atmospheric mass after 1 Gyr for cases with a range of planetary and initial atmospheric masses, assuming the planets are orbiting a slow rotator (*left-panel*) and a fast rotator (*right-panel*). In both panels, dark red and white corresponds to 100% and 0% respectively of the initial atmospheric mass remaining. The grey areas in the upper left corners show areas of parameter space that are unphysical. The shaded black areas show the range of estimates by Stökl *et al.* (2016) for how massive an atmosphere the planets would pick up from the gas disk after 10,000 years (lower boundary) and 1 Myr (upper boundary).

interactions with the surface). As discussed in Section 2.3, the evolution of the activity of solar mass stars can be very different depending on the initial rotation rate of the host star. Tu *et al.* (2015) and Johnstone *et al.* (2015b) studied how these different activity evolution tracks would lead to different evolutions of a terrestrial planet orbiting these stars. Johnstone *et al.* (2015b) calculated a grid of atmospheric evolution models for different planetary and initial atmospheric masses, and their results are summarised here in Fig. 6. For Earth mass planets, they found that when the planets start out (at 10 Myr) with masses of $\sim 1\%$ of the Earth mass, as estimated by Stökl *et al.* (2016), the subsequent atmospheric evolution will be very different for different stellar rotation tracks. If the planet orbits a rapid rotator, the planet loses all of its atmosphere in ~ 300 Myr. If the planet orbits a slow rotator, the planet only loses about half of its atmosphere by 1 Gyr; after this, the atmosphere likely remains for the entire lifetime of the planet due to the low activity of the host star. On the other hand, if the planet starts out with a less massive atmosphere of $\sim 0.1\%$ of the Earth mass (such as can happen if

the planet only grows to a fraction of its final mass during the phase), the atmosphere will be completely eroded in both cases, but the timescale depends sensitively on the star's initial rotation rate. The lower panels of Fig. 6 show the fraction of the atmosphere remaining after 1 Gyr for all models, with the black shaded area showing the range of estimates for the initial atmospheric mass estimated by Stökl *et al.* (2016).

5. Final remarks

The effects I discuss in this review are primarily related to stellar XUV radiation and winds, and I mostly ignore the effects of energetic (i.e. fast moving) particles. Such particles have several sources, including the solar corona, shocks propagating through the inner heliosphere, the planet's own magnetosphere, and from outside the solar system (i.e. galactic cosmic rays). The multitude of ways in which they can influence atmospheres is not discussed here, largely due to lack of space and expertise on the part of the author, and not because they are any less important and interesting than the effects that are discussed. I have also ignored the influences that impacts of larger bodies, ranging from small asteroids up to protoplanets, can have on atmospheric loss, which is expected to be especially important early in a planet's evolution.

6. Acknowledgements

The author acknowledges the support of Austrian Science Fund (FWF) NFN project S11601-N16 "Pathways to Habitability: From Disk to Active Stars, Planets and Life" (path.univie.ac.at/) and the related subproject S11604-N16, and also the International Space Science Institute (ISSI) team "The Early Evolution of the Atmospheres of Earth, Venus, and Mars", supported by ISSI.

References

- Aarnio, A. N., Matt, S. P., & Stassun, K. G. 2012, *ApJ* 760 9
- Abbo, L., Ofman, L., Antiochos, S. K., Hansteen, V. H., Harra, L., Ko, Y.-K., Lapenta, G., Li, B., Riley, P., Strachan, L., von Steiger, R., & Wang, Y.-M. 2016, *SSRv* 201 55
- Airapetian, V. S. & Usmanov, A. V. 2016, *ApJ*, 817 24
- Bouvier, J., Matt, S. P., Mohanty, S., Scholz, A., Stassun, K. G., & Zanni, C. 2014, *Protostars and Planets VI. Univ. Arizona Press, Tucson, AZ*, p. 433
- Chassefière, E. 1997, *Icar*, 126 229
- Cohen, O., Ma, Y., Drake, J. J., Gloer, A., Garraffo, C., Bell, J. M., & Gombosi, T. I. 2015, *ApJ*, 806 41
- Cohen, O., Yadav, R., Garraffo, C., Saar, S. H., Wolk, S. J., Kashyap, V. L., Drake, J. J., & Pillitteri, I. 2016, *ApJ*, (accepted)
- Cranmer, S. R. 2009, *LRSP*, 6 3
- Cranmer, S. R. & Saar, S. H. 2009, *ApJ*, 741 54
- Eddy, J. A. & Ise, R. 1979, *Book: A new sun : the solar results from SKYLAB*
- Ehrenreich, D., Lecavelier Des Etangs, A., Hébrard, G., Désert, J.-M., Vidal-Madjar, A., McConnell, J. C., Parkinson, C. D., Ballester, G. E., & Ferlet, R. 2008, *A&A*, 483 933
- Elkins-Tanton, L. T. 2008, *EGPSL*, 271 181
- Fontenla, J. M., Curdt, W., Haberleiter, M., Harder, J., & Tian, H. 2009, *ApJ*, 707 482
- Fontenla, J. M., Linsky, J. L., Witbrod, J., France, K., Buccino, A., Mauas, P., Vieytes, M., & Walkowicz, L. M. 2016, *ApJ*, 830 154
- Fontenla, J. M., Harder, J., Livingston, W., Snow, M., & Woods, T. 2011, *JGRD*, 11620108F
- Gaidos, E. J., Güdel, M., & Blake, G. A. 2000, *GeoRL*, 27 501
- Gloer, A., Tóth, G., Ma, Y., Gombosi, T., Zhang, J.-C., & Kistler, L. M. 2009, *JGRA*, 11412203

- Güdel, M., Guinan, E. F., & Skinner, S. L. 1997, *ApJ*, 483 947
- Gunell, H., Brinkfeldt, K., Holmström, M., Brandt, P. C. :, Barabash, S., Kallio, E., Ekenbäck, A., Futaana, Y., Lundin, R., Andersson, H. *et al.* 2006, *Icar*, 182 431
- Johnson, R. E. 1994, *SSRv*, 69 215
- Johnstone, C. P., Güdel, M., Lüftinger, T., Toth, G., & Brott, I. 2015a, *A&A*, 577 27
- Johnstone, C. P., Güdel, M., Brott, I., & Lüftinger, T. 2015b, *A&A*, 577 28
- Johnstone, C. P., Güdel, M., Stökl, A., Lammer, H., Tu, L., Kislyakova, K. G., Lüftinger, T., Odert, P., Erkaev, N. V., & Dorfi, E. A. 2015b, *ApJ*, 815 12
- Johnstone, C. P. & Güdel, M. 2015, *A&A*, 578 129
- Johnstone, C. P. 2016, *A&A*, (accepted)
- Kislyakova, K. G., Johnstone, C. P., Odert, P., Erkaev, N. V., Lammer, H., Lüftinger, T., Holmström, M., Khodachenko, M. L., & Güdel, M. 2014, *A&A*, 562 116
- Kislyakova, K. G., Holmström, M., Lammer, H., Odert, P., & Khodachenko, M. L. 2014, *Science*, 346 981
- Kislyakova, K. G., Fossati, L., Johnstone, C. P., Holmström, M., Zaitsev, V. V., & Lammer, H. 2015, *ApJ*, 799 15
- Kleine, T., Touboul, M., Bourdon, B., Nimmo, F., Mezger, K., Palme, H., Jacobsen, S. B., Yin, Q.-Z., & Halliday, A. N. 2009, *GeCoA*, 73 5150
- Lammer, H., Kasting, J. F., Chassefière, E., Johnson, R. E., Kulikov, Y. N., & Tian, F. 2009, *SSRv*, 139 399
- Lammer, H., Stökl, A., Erkaev, N. V., Dorfi, E. A., Odert, P., Güdel, M., Kulikov, Y. N., Kislyakova, K. G., & Leitzinger, M. 2014, *MNRAS*, 439 3225
- Lichtenegger, H. I. M., Kislyakova, K. G., Odert, P., Erkaev, N. V., Lammer, H., Gröller, H., Johnstone, C. P., Elkins-Tanton, L., Tu, L., Güdel, M., & Holmström, M. 2016, *JGRA*, 121 4718
- Luhmann, J. G. & Kozyra, J. U. 1991, *JGR*, 96 5457
- Owen, J. E. & Wu, Y. 2016, *ApJ*, 817 1070
- Owen, J. E. & Mohanty, S. 2016, *MNRAS*, 459 40880
- Pevtsov, A. A., Fisher, G. H., Acton, L. W., Longcope, D. W., Johns-Krull, C. M., Kankelborg, C. C., & Metcalf, T. R. 2003, *ApJ*, 598 1387
- Pizzolato, N., Maggio, A., Micela, G., Sciortino, S., & Ventura, P. 2003, *A&A*, 397 147
- Ribas, I., Guinan, E. F., Güdel, M., & Audard, M. 2005, *ApJ*, 622 680
- Robbrecht, E., Berghmans, D., & Van der Linden, R. A. M. 2009, *ApJ*, 691 1222
- Rogers, L. A. 2015, *ApJ*, 801 41
- Stökl, A., Dorfi, E., & Lammer, H. 2015, *A&A*, 576 87
- Stökl, A., Dorfi, E. A., Johnstone, C. P., & Lammer, H. 2016, *ApJ*, 825 86
- Tian, F., Kasting, J. F., Liu, H.-L., & Roble, R. G. 2008, *JGRE*, 113 5008
- Tu, L., Johnstone, C. P., & Güdel, M., Lammer 2015, *A&A*, 577 L3
- van der Holst, B., Sokolov, I. V., Meng, X., Jin, M., Manchester, IV, W. B., Tóth, G., & Gombosi, T. I. 2014, *ApJ*, 782 81
- Vidotto, A. A., Fares, R., Jardine, M., Moutou, C., & Donati, J.-F. 2015, *MNRAS*, 449 4117
- Wang, Y. & Zhang, J. 2007, *AJ*, 665 1428
- West, A. A., Hawley, S. L., Bochanski, J. J., Covey, K. R., Reid, I. N., Dhital, S., Hilton, E. J., & Masuda, M. 2008, *AJ*, 135 785
- Wood, B. E., Müller, H.-R., Redfield, S., Edelman, E. 2014, *ApJ*, 781 33